Supplementary Materials for

The Mechanism of MICU-Dependent Gating of the Mitochondrial Ca^{2+} Uniporter

Vivek Garg*, Ishan Paranjpe, Tiffany Unsulangi, Junji Suzuki, Lorin S. Milescu, and Yuriy Kirichok*.

*Correspondence to: yuriy.kirichok@ucsf.edu (YK); vivek.garg@ucsf.edu (VG)

This PDF file includes:

MATERIALS AND METHODS

Cell culture and recombinant gene expression

All mouse embryonic fibroblast (MEF) cells with (*32*) or without Drp1 (*46*), and all knockout clones were grown in low glucose (5.6 mM) Dulbecco's modified Eagle's medium (DMEM) supplemented with 10% FBS, 100 U/ml penicillin, and 100 U/ml streptomycin at 37°C, 5% CO_2. Cells were maintained by splitting every 48-72 hours at a ratio of 1:5 to 1:10.

We used third generation lentiviral (bi-cistronic) vectors containing the ORF for gene of interest with or without a selection marker (EGFP, mCherry or puromycin, Supplementary Fig. 1 and 2). The vectors were generated by VectorBuilder, Inc. (Chicago, IL, USA), and their sequences were confirmed independently by the company and by us. Recombinant cDNA expressing cells were enriched using multiple rounds of FACS or antibiotic selection. In some cases, EGFP was targeted to mitochondria (using a mitochondrial targeting sequence from COX8) to identify mitoplasts expressing the recombinant protein of interest during patch clamp experiments.

Quantitative Real-Time PCR Analysis

qPCR was performed by Syd Labs (Natick, MA, USA). Total RNA was isolated from cells using the RNAeasy Minikit (QIAGEN), and reverse transcribed using the First Strand cDNA Synthesis Kit (Syd Labs). qPCR reactions were performed with the following gene-specific primers (generated by Integrated DNA Technologies):

Hprt,	Forward Primer	5'-GTCCCAGCGTCGTGATTAGC-3'
	Reverse Primer	5'-GTGATGGCCTCCCATCTCCT-3'
MCU,	Forward Primer	5'-AAGGGCTTAGCGAGTCTTGTC-3'
	Reverse Primer	5'- GGGTGCTGGTGTGTTAGTGT -3'
MCUb,	Forward Primer	5'-CCACACCCCAGGTTTTATGTATG-3'
	Reverse Primer	5'-ATGGCAGAGTGAGGGTTACCA-3'
EMRE,	Forward Primer	5'-ATTTTGCCCAAGCCGGTGAA-3'
	Reverse Primer	5'-CCTCAAGCAGAGCAGCGAAG-3'
MICU1,	Forward Primer	5'-CTTAACACCCTTTCTGCGTTGG-3'
	Reverse Primer	5'-AGCATCAATCTTCGTTTGGTCT-3'
MICU2,	Forward Primer	5'-CTCCGCAAACAGCGGTTCAT-3'
	Reverse Primer	5'-TGCCAGCTTCTTGACCAGTG-3'
MICU3,	Forward Primer	5'-GTAAGGTCAGAGCACGCAGAA-3'
	Reverse Primer	5'-TTTCCTGTTGGACGCTGACAA -3'

cDNA (100 ng, calculated from initial RNA) samples were pre-amplified for 12 cycles using ABsolute qPCR SYBR Green Low ROX Mix (ThermoFisher). qPCR reactions were performed using an Agilent MX3000 (Fluidigm) with 40 cycles of amplification (15 s at 95°C, 5 s at 70°C, and 60 s at 60°C). Ct values were calculated by the Real-Time PCR Analysis Software (Fluidigm). Relative gene expression was determined by the ΔCt method. Hprt was selected as the reference gene.

Generation of knockout cell lines by the CRISPR/Cas9 method

Knockout MEF cell lines were generated using the CRISPR/Cas9 method (*70*). All knockouts (except the *MCU*$^{-/-}$ line) were generated by Alstem LLC (Richmond, CA, USA). Either one sgRNA or a pair of two adjacent sgRNAs were used to create a point indel or a truncate indel, respectively (Fig. S1).

MCU,	TGGCAGCGCTCGCGTCGAGA GGG
EMRE,	GAGTGTCCCGACATAGAGAA AGG
	CTTACACTCCCACTAGGTTA AGG
MICU1,	TCACTTTTAGATGCTGCCGG TGG
	CTGCAAGTACCGGTCTCCTG TGG
MICU2,	CGTTCGGGAGCCCTCGCGCG CGG
	GGGCGCTTCCGCAAAGATGG CGG
MICU3,	GGGCGAGCTGAGCATCGCGG CGG
	CCGGGGCCGCTAGCTCCGAG GGG

MEFs were transfected with the Cas9 gRNA vector (Addgene: PX459) via electroporation (Invitrogen Neon transfection system) using the following parameters: 1×10^6 cells and 1 µg of two different gRNA-Cas9 plasmids. Puromycin was used for enrichment of transfected cells, and serial dilution was performed to select single-cell clones. A stable homozygous knockout cell line was confirmed by PCR amplification of the targeted region, cloning into a pUC19 vector, and sequencing showing that either a frameshift or large deletion had occurred in the targeted region of the gene (Fig. S1). All knockout clones were further validated by Western blotting (Fig. S2). The primers used for amplification of genomic sites and cloning into pUC19 sequencing vector were as follows:

MCU,	Forward Primer	TAGAAGCTTTCCACTGCTCTGATTGATCTTG
	Reverse Primer	ATGTGAATTCGAGCTGCTTTGGAATGAGAC
EMRE,	Forward Primer	GTGAAGCTTGGGATCAGTAGTCCATTGGAGG
	Reverse Primer	AGGAGAATTCAGTGAGAGTTCCTGTGGTATG
MICU1,	Forward Primer	TTTAAGCTTGATTCCTTTGAGTTATAAGTAG
	Reverse Primer	CAAAGAATTCAGCAAAGAAATTCTGATGTA
MICU2,	Forward Primer	ACCAAGCTTGAACGTCGAGGAAGCAGCCAC
	Reverse Primer	AGGAGAATTCTCCATCCACCAGGTGGGCAG
MICU3,	Forward Primer	CGCAAGCTTCTCGCGAGATTTCGGCCCGCC
	Reverse Primer	AGGAGAATTCTCCATCCACCAGGTGGGCAG

Isolation of mitochondria and mitoplasts from MEFs

Mitoplasts were isolated from MEFs using methodology previously described (*41*). Briefly, MEFs were homogenized in ice-cold medium (Initial medium) containing 250 mM sucrose, 10 mM HEPES, 1 mM EGTA, and 0.1% bovine serum albumin (BSA) (pH adjusted to 7.2 with Trizma® base) using a glass grinder with six slow strokes of a Teflon pestle rotating at 280 rpm. The homogenate was centrifuged at 700× g for 10 min to create a pellet of nuclei and unbroken cells. The first nuclear pellet was resuspended in the fresh Initial medium and homogenized again to increase the mitochondrial yield. Mitochondria were collected by centrifugation of the supernatant at 8,500× g for 10 min.

Mitoplasts were produced from mitochondria using a French press. Mitochondria were suspended in a hypertonic solution containing 140 mM sucrose, 440 mM D-mannitol, 5 mM HEPES, and 1 mM EGTA (pH adjusted to 7.2 with Trizma® base) and then subjected to a French press at 1,200–2,000 psi to rupture the outer membrane. Mitoplasts were pelleted at 10,500× g for 15 min and resuspended for storage in 0.5–1 ml of solution containing 750 mM KCl, 100 mM HEPES, and 1 mM EGTA (pH adjusted to 7.2 with Trizma® base). Mitoplasts prepared and stored with this method contained the same amount of auxiliary MICU1 and MICU2 subunits as compared to intact mitochondria (Fig. S4a, see the co-immunoprecipitation section below).

Mitochondria and mitoplasts were prepared at 0–4 °C and stored on ice for up to 5 h. Immediately before the electrophysiological experiments, 15–50 µl of the mitoplast suspension was added to 500 µl solution containing 150 mM KCl, 10 mM HEPES, and 1 mM EGTA (pH adjusted to 7.0 with Trizma® base) plating on 5-mm coverslips pretreated with 0.1% gelatin to reduce mitoplast adhesion.

Patch-clamp recording

Whole mitoplast currents were measured as described previously (*41*). Gigaohm seals with mitoplasts were formed in the bath solution containing 150 mM KCl, 10 mM HEPES and 1 mM EGTA, pH 7.2 (adjusted with KOH). Voltage steps of 350–500 mV for 2-8 ms were applied to rupture the IMM and obtain the whole-mitoplast configuration. Typically, pipettes had resistances of 20–40 MΩ, and the access resistance was 35–65 MΩ. The membrane capacitances of mitoplasts range from 0.2 – 0.6 pF.

All indicated voltages are on the matrix side of the IMM (pipette solution), relative to the cytosolic side (bath solution, Fig. S3) (*41*). Currents were normally induced by a voltage ramp from -160 mV to +80 mV (interval between pulses was 5 s) to cover all physiological voltages across the IMM, but other voltage protocols were also used as indicated in the figures. All whole-IMM recordings were performed under continuous perfusion of the bath solution. Currents were normalized per membrane capacitance to obtain current densities (pA/pF). Currents flowing into mitochondria are shown as negative, while those flowing out are positive. Membrane capacitance transients observed upon application of voltage steps were removed from current traces.

Typically, pipettes were filled with one of the following three solutions (*41*) (tonicity was adjusted to ~350 mmol/kg with sucrose.):

Solution A was used to measure I_{Ca} and contained: 110 mM Na-gluconate, 40 mM HEPES, 10 mM EGTA and 2 mM $MgCl_2$ (pH 7.0 with NaOH)

Solution B was used to measure I_{Na} or I_{Mn} and contained: 110 Na-gluconate, 40 HEPES, 1 EGTA, 5 EDTA and 2 mM NaCl (pH 7.0 with Tris base).

Solution C was used to measure outward I_{Ca} (the MCU rectification experiments) and contained: 130 mM tetramethylammonium hydroxide (TMA), 100 mM HEPES and 2 mM $CaCl_2$ (pH 7.0 with D-gluconic acid)

To measure whole-mitoplast I_{Ca}, the bath solution was formulated to contain only 150 mM HEPES (pH 7.0 with Tris base, tonicity ~300 mmol/kg with sucrose) and different dilutions of $CaCl_2$ from a 1 M stock (Sigma)(*9*). The control solution contained: 150 mM HEPES, 80 mM sucrose and 1 mM EGTA (pH 7.0 with Tris base, tonicity ~300 mmol/kg with sucrose). The bath solution used for measuring I_{Na} contained: 110 mM Na-gluconate, 40 mM HEPES, 1 mM EGTA and 5 mM EDTA (pH 7.0 with Tris base, tonicity ~300 mmol/kg with sucrose). The bath

solution for measuring inhibition of I_{Na} by cytosolic Ca^{2+} contained: 110 mM Na-gluconate, 40 mM HEPES and 10 mM EDTA (pH 8.0 with Tris, tonicity ~380 mmol/kg with sucrose)) and varying amounts of $CaCl_2$ were added to the bath solution to achieve the free [Ca^{2+}] calculated using the MaxChelator program (C. Patton, Stanford University).

A rapid exchange of $[Ca^{2+}]_{cyto}$ from virtual zero (control solution) to 1 mM was achieved using a commercially available piezo-driven, fast solution exchange system (Warner Instruments, SF-77B perfusion fast step system). It was interfaced with our pClamp acquisition software in order to precisely time the steps during solution change. The timing (τ ~0.4 ms) for solution exchange was judged by the current changes because of a junction potential difference using solutions with different ionic strengths.

Currents were recorded using an Axopatch 200B amplifier (Molecular Devices). Data acquisition and analyses were performed using PClamp 10 (Molecular Devices) and Origin 9.6 (OriginLab). All data were acquired at 10 kHz and filtered at 1 kHz.

Single-channel recordings and analysis

All single-channel data were acquired from inside–out patches excised from isolated mitoplasts(*9*). Patches were excised in a bath solution containing 150 mM KCl, 10 mM HEPES and 1 mM EGTA, pH 7.2 (adjusted with KOH). Recordings were performed under symmetrical conditions (the same bath and pipette solutions): 105 mM $CaCl_2$ and 40 mM HEPES, pH 7.0 with Tris base. Signals were sampled at 50 kHz and low-pass filtered at 1 kHz. Fire-polished, borosilicate pipettes (Sutter QF-150-75) coated with Silguard (Dow Corning Corp., Midland, MI) and having a tip resistance of 50–70 MΩ were used for low noise recordings.

To characterize the single-channel conductance and subconductance levels and their occupancy probabilities, we used the MLab version of the QuB software, freely available from the Milescu lab at: https://milesculabs.biology.missouri.edu/QuB_Downloads.html. The data were first resampled at 2.5 kHz and then were idealized with the Baum-Welch and Viterbi algorithms, as implemented in QuB, which classify each point in the data to a conductance level and produce estimates of current amplitudes and occupancy probabilities. The time-averaged single-channel current can be calculated as the product between occupancy probability and current amplitude, summated over all conductance levels (main open state and substates).

Time-lapse Ca^{2+} imaging

For imaging experiments, MEFs were plated on collagen type-I-coated glass-bottom 35 mm dishes (P35G-1.5-14-C, Matek), 48–72 h before imaging. Cells were imaged at the interval of 3 s on a Nikon Ti-E microscope using a 40× objective (NA 1.30, oil, CFI Plan Fluor, Nikon), Lambda 421 LED light source (Sutter) and ORCA Flash 4.0 CMOS camera (Hamamatsu Photonics) at room temperature (25°C). The following excitation/emission filter settings were used: 340±13 nm/525±25 and 389±19 nm/510±40 for cytosolic Ca^{2+} imaging using fura-2 (K_d=224 nM) and 480±40 nm nm/525±15 nm for mitochondrially targeted *cepia2* (*CEPIA2mt*, K_d=160 nM (*47*), cloned into a lentiviral vector). Cells were loaded with 3 μM fura-2 AM (Life Tech., USA) in DMEM/FBS at room temperature for 30 min. After three washes with physiological salt solution (PSS) containing (in mM) 150 NaCl, 4 KCl, 2 $CaCl_2$, 1 $MgCl_2$, 5.6 glucose and 25 HEPES (pH 7.4), each dish was placed on the stage for imaging. Imaging was performed in PSS within 1 h of dye staining. Baseline fluorescence was taken for 1–2 min after which thapsigargin (Tg) (final [Tg] = 300 nM) was added while imaging was continued for another 10–15 min.

Fura-2 Calibration: Baseline measurements were taken, and cells were incubated in PSS (No $CaCl_2$) containing 3 mM EGTA, 1 μM ionomycin and 1 μM Tg for 5–10 min. After 2–3 washes with PSS (No $CaCl_2$) containing 0.3 mM EGTA, cells were imaged for 5 min (average of last 10 frames was used for calculation) to obtain the R_{min} and F_{380max} values. Finally, PSS containing 10 mM $CaCl_2$ (no EGTA), 1 μM ionomycin and 1 μM Tg was added and cells were imaged for 10 min. After the signal reached saturation (~3 min), the average value from 10 frames was used to calculate R_{max} and F_{380min} values. Using these obtained values, the fura-2 ratio was calibrated by the following equation (*71*):

$$[Ca^{2+}]free = K_d * \left(\frac{[R - Rmin]}{[Rmax - R]}\right) * (F_{380max}/F_{380min})$$

All image analyses were done with ImageJ (NIH). Briefly, mitochondrial and cytosolic regions were manually determined for each cell. The average fluorescence intensity in the regions was measured and the background intensity was subtracted. For analysis of the *cepia2* signal, we normalized the fluorescence intensity by the baseline fluorescence. For analysis of the fura-2 signal, we calculated the fluorescence ratio (F_{340}/F_{380} for fura-2).

The time point for increase in mitochondrial $[Ca^{2+}]$ (upstroke) was detected using a script written in Python and manually checked afterwards. Briefly, the fluorescence signal was smoothed by applying a second–order zero phase digital Butterworth filter with an optimal cutoff frequency as previously described (*72*). From the smoothed signal, the upstroke frame was defined as the earliest point between the baseline and signal peak that was greater than 80% of the maximal time derivative. The time-point for change in mitochondrial signal was time-matched with the fura-2 reading to determine the threshold $[Ca^{2+}]_{cyto}$.

Co-immunoprecipitation

Mitochondria or mitoplasts were isolated from MEFs deficient in the MCU subunit but stably expressing Flag-tagged MCU. Mitochondrial fraction from wild type cells (without MCU-FLAG) was used as negative control. Isolated mitoplasts (but not mitochondria) were incubated in 750 mM KCl for 30 min before solubilization. Briefly, 300 μg of protein lysate was solubilized with 500 μl of lysis buffer (50 mM HEPES pH 7.4, 150 mM NaCl, 1 mM EGTA, 0.2% DDM and Halt protease inhibitor cocktail [Thermo Fisher]) for 30 min at 4°C. Lysates were cleared by spinning at 20,000× g for 10 min at 4°C. Cleared lysates were incubated with anti-Flag M2 affinity gel (Sigma A2220) for 2 h at 4°C. Immunoprecipitates were washed with 1 ml of lysis buffer three times and boiled in 20 μl of Laemmli buffer (without β-mercaptoethanol). One-third of the immunoprecipitate was loaded onto a 4–20% gradient SDS-PAGE gel for detection of the indicated proteins by Western blotting. Flow-through fraction was also collected and analyzed in the same gel.

Immunoblots

For Western blot analysis, MEFs or isolated mitochondria/mitoplasts were lysed in radioimmunoprecipitation assay (RIPA) buffer (1% IGEPAL®, 0.1% sodium dodecyl sulfate, 0.5% sodium deoxycholate, 150 mM NaCl, 1 mM EDTA, 50 mM Tris-HCl (pH 7.4) and a cocktail of proteases inhibitors). Lysates were resolved by SDS-PAGE; transferred to PVDF membrane (Millipore); and probed with anti-MCU (Sigma, HPA016480, 1:2,000), anti-EMRE (Santa Cruz, sc-86337, 1:200), anti-HSP60 (Santa Cruz, sc-1052, 1:3,000), anti-VDAC (Abcam, ab15895, 1:2,000), anti-MICU1 (Cell Signaling Technology, 12524S, 1:2,000), anti-MICU2 (Bethyl, A300-BL19212, 1:500), anti-MICU3 (Sigma, HPA024779, 1:1,000) and anti-TOM20 (Santa Cruz, sc-11415, 1:2,000). Anti-MICU1 antibody produced a non-specific band near its

monomeric molecular weight (~50 kDa), so samples were prepared in Laemmli buffer without β-mercaptoethanol to detect MICU1 homo- or hetero-dimers (~100 kDa).

Statistical analysis

Data are presented as mean ± standard error of the mean (SEM), as specified in the figure legend. Statistical analysis was completed in Excel or Origin 9.6. All experiments were performed in triplicate or more. Statistical significance at an exact *p-value* was determined with the methods as indicated in the corresponding figure legends.

SUPPLEMENTARY FIGURES

Fig. S1. Generation of knockouts for various MCU complex subunits. (**A**) A schematic arrangement of various subunits in the MCU complex. Four MCU and four EMRE subunits form the pore of the MCU complex (only two MCU and two EMRE subunits are shown for simplicity). EMRE also tethers MICU1 subunit to the pore on the cytosolic side of the IMM (i.e., in the mitochondrial intermembrane space, IMS). MICU1 forms homodimers or hetero-dimerizes with MICU2 or MICU3 (not shown). Each MICU subunit has two EF hands that bind cytosolic Ca^{2+}. (**B** to **F**) CRISPR-mediated indels in various MCU subunit genes and the resulting mutant alleles. The CRISPR binding sites (for sgRNA) are highlighted in *yellow*, and their PAM sequences are highlighted in *green*. The translational initiation codon (ATG) is shown in *bold* where applicable. (B) Overview of the *MCU* gene and indels in the knockout. A sgRNA was used to target exon 3. The sequence of targeted region in MCU gene is shown; exon 3 is underlined. Targeted sequencing indicates frame-shift indels (*red*) in both alleles (*Al*-1 and *Al*-2). (C) Overview of the *EMRE* gene and truncated region in the knockout. Two sgRNAs were used for CRISPR-Cas9–mediated deletion in the exon-2 (*underlined*) and the flanking region. Targeted sequencing indicates same 259-bp deletion (*red*) in both alleles. (D) Overview of the *MICU1* gene and truncated region in the knockout. Two sgRNAs were used for CRISPR-Cas9–mediated deletion in the exon-3 (*underlined*) and the flanking region. Targeted sequencing indicates that almost all of exon-3 is deleted along with a portion of the flanking region (*red*) in both alleles (*Al*-1 and A*l*-2). (E) Overview of the *MICU2* gene and truncated region in the knockout. Two sgRNAs were used for CRISPR-Cas9–mediated deletion in the exon-1 (*underlined*) and the flanking region. Targeted sequencing indicates that almost all of exon-1 is deleted (*red*) in both alleles. (F) Overview of the *MICU3* gene and truncated region in the knockout. Two sgRNAs were used for CRISPR-Cas9–mediated deletion in the exon-1 (*underlined*). Targeted sequencing indicates a 73-bp deletion in the expected cut area (*red*) in both alleles.

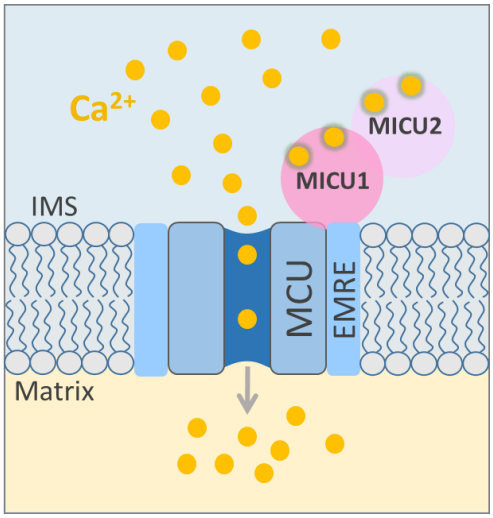

MCU complex model

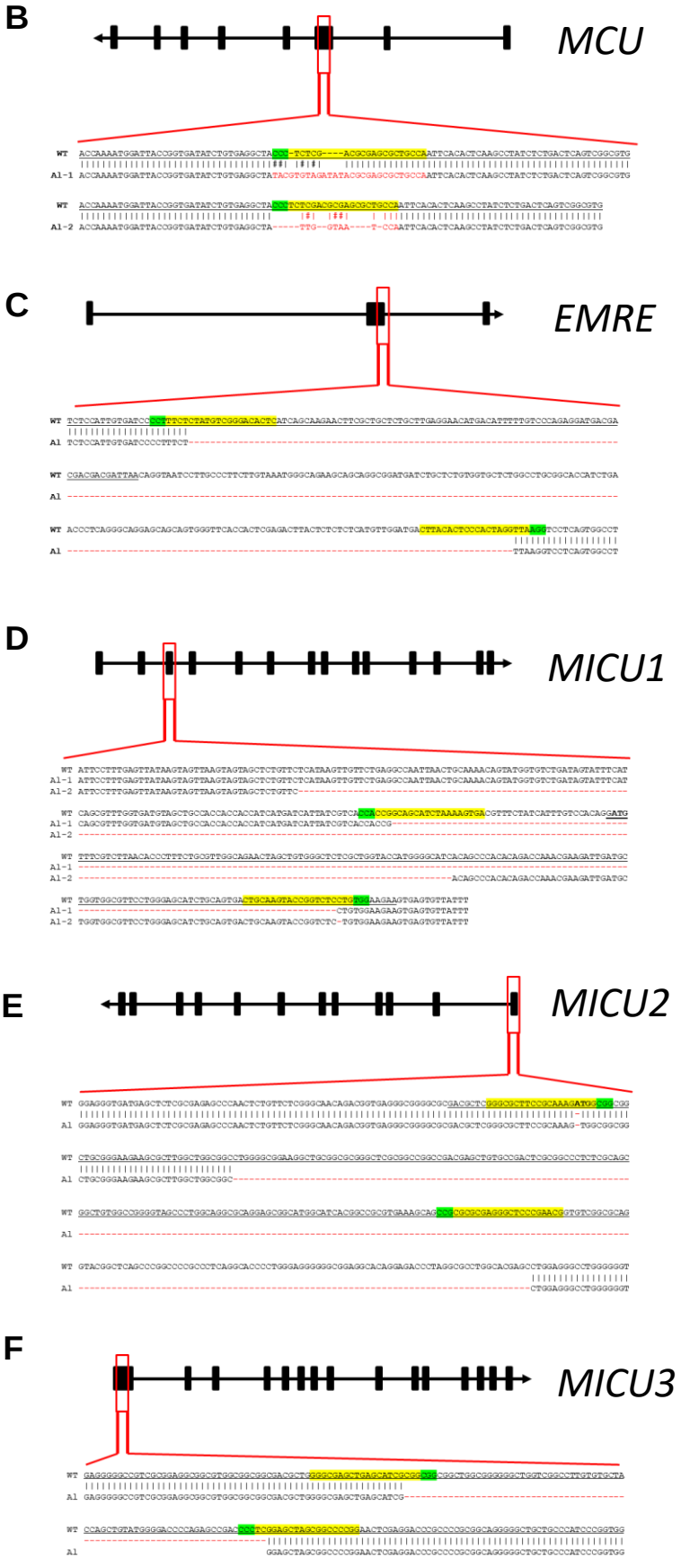

Fig. S1

Fig. S2. Expression of various MCU complex subunits and $[Ca^{2+}]_{mito}$ phenotype in cells deficient for various MCU complex subunits. (**A** to **C**) Western blots show expression of various MCU complex subunits in the respective knockout cells. For MICU1 (**A**), samples were prepared without reducing agent, β-mercaptoethanol. The MICU1 band is near the expected molecular weight (~100 kDa) for the homo- or hetero-dimer (with MICU2 or 3). Multiple bands were observed with anti-MICU2 (**B**) and anti-MICU3 (**C**) antibodies, which were absent in knockout cell lines. This is likely due to the presence of different oligomeric states of the protein, as well as the mature and nascent (before truncation of the mitochondrial targeting signal) forms of the protein. Arrows mark the mature (m) and nascent (n) proteins near the expected molecular weight. (**D**) PCR showing the mRNA expression of various MCU subunits in *Drp1*$^{-/-}$ MEFs. Hprt was used as the reference. (**E** to **J**) Representative $[Ca^{2+}]_{mito}$ (*black*, left ordinate) and $[Ca^{2+}]_{cyto}$ (*blue*, right ordinate) in an individual cell with *WT* MCU complex, and individual cells with MCU, EMRE, and MICU1–3 knockouts before and after application of 300 nM Tg (arrow). Dashed red lines indicate the $[Ca^{2+}]_{cyto}$ at which the $[Ca^{2+}]_{mito}$ starts to increase ("$[Ca^{2+}]_{cyto}$ threshold"). (**K** to **M**) Resting $[Ca^{2+}]_{cyto}$ (K), peak $[Ca^{2+}]_{cyto}$ after addition of Tg (L), and $[Ca^{2+}]_{cyto}$ threshold for $[Ca^{2+}]_{mito}$ elevation (M) in *WT* and indicated knockout cell lines. *WT* (n = 5 dishes, total cells = 150); *MCU*$^{-/-}$ (n = 3 dishes, total cells = 183); *EMRE*$^{-/-}$ (n = 4 dishes, total cells = 187); *MICU1*$^{-/-}$ (n = 4 dishes, total cells = 196); *MICU2*$^{-/-}$ (n = 4 dishes, total cells = 192); and *MICU3*$^{-/-}$ (n = 3 dishes, total cells = 115). Mean ± SEM; one-way ANOVA with post-hoc Tukey test. *p< 0.05; ***p< 0.001. Statistics was run on number of dishes.

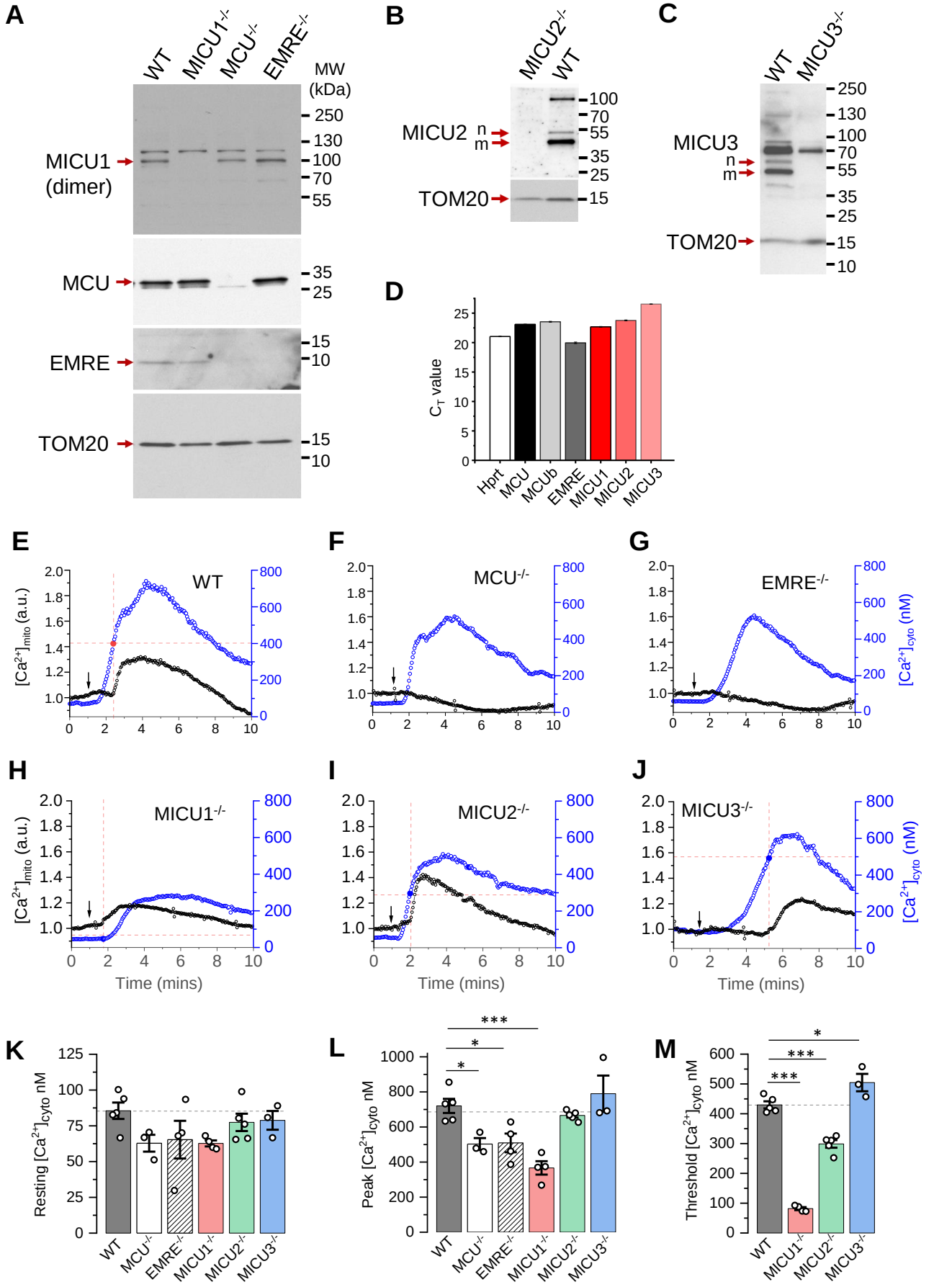
A
WT
MICU1-/-
MCU-/-
EMRE-/-
MW (kDa)
MICU1 (dimer)
MCU
EMRE
TOM20
B
MICU2-/-
WT
MICU2
n
m
TOM20
C
WT
MICU3-/-
MICU3
n
m
TOM20
D
CT value
Hprt
MCU
MCUb
EMRE
MICU1
MICU2
MICU3
E
WT
F
MCU-/-
G
EMRE-/-
H
MICU1-/-
I
MICU2-/-
J
MICU3-/-
[Ca2+]mito (a.u.)
[Ca2+]cyto (nM)
Time (mins)
K
Resting [Ca2+]cyto nM
L
Peak [Ca2+]cyto nM
M
Threshold [Ca2+]cyto nM

Fig. S2

Fig. S3. Recording MCU currents across the whole IMM. (**A**) Diagram of patch-clamp recording from a vesicle of the whole IMM (mitoplast). After formation of a gigaohm seal between the patch pipette and the mitoplast, the IMM patch under the pipette is broken by applying short pulses of high voltage (200–500 mV, 2–8 ms), sometimes combined with light suction, to gain access into the mitoplast through the pipette. In this configuration, called the "whole-IMM" configuration, the interior of the mitoplast (mitochondrial matrix) is perfused with the pipette solution. The bath is also perfused to control the experimental solution on the cytosolic side of the IMM. The voltage across the IMM is set to the desired value (V), and the currents (I) are measured using the patch-clamp amplifier. Directions of currents flowing across the IMM: inward currents (flowing into the mitoplast) are negative, while outward currents are positive. (**B**) *Left panel:* Example MCU current traces recorded in the whole-IMM configuration. The voltage protocol used to elicit the currents is shown above. All indicated voltages are within the mitochondrial matrix relative to the bath (cytosol). The voltage of the bath solution is defined to be zero. The zero current level is shown by the dashed line and an arrow. The directions of the currents are indicated as negative (inward) and positive (outward). The MCU current in Ca^{2+}-free bath solution (control) is shown in *grey*. The outward current in control is mediated by Na^+ ions permeating through the MCU channel in the Ca^{2+}-free conditions (I_{Na}, pipette solution contains Na^+). After application of 1 mM Ca^{2+} on the cytosolic face of the IMM (bath), we observe an inward Ca^{2+} current (I_{Ca}, *blue*) via MCU, while the outward I_{Na} is simultaneously inhibited. *Right panel*, When $[Ca^{2+}]_{cyto}$ is brought to virtual zero (1 mM EGTA and 5 mM EDTA) under conditions when both bath and pipette solution contain Na^+, we observe I_{Na} via MCU (*red*) in both inward and outward directions. The current amplitude and time calibration bars are indicated. The current amplitude is normalized per membrane capacitance to facilitate comparison of current amplitudes between mitoplasts of different sizes.

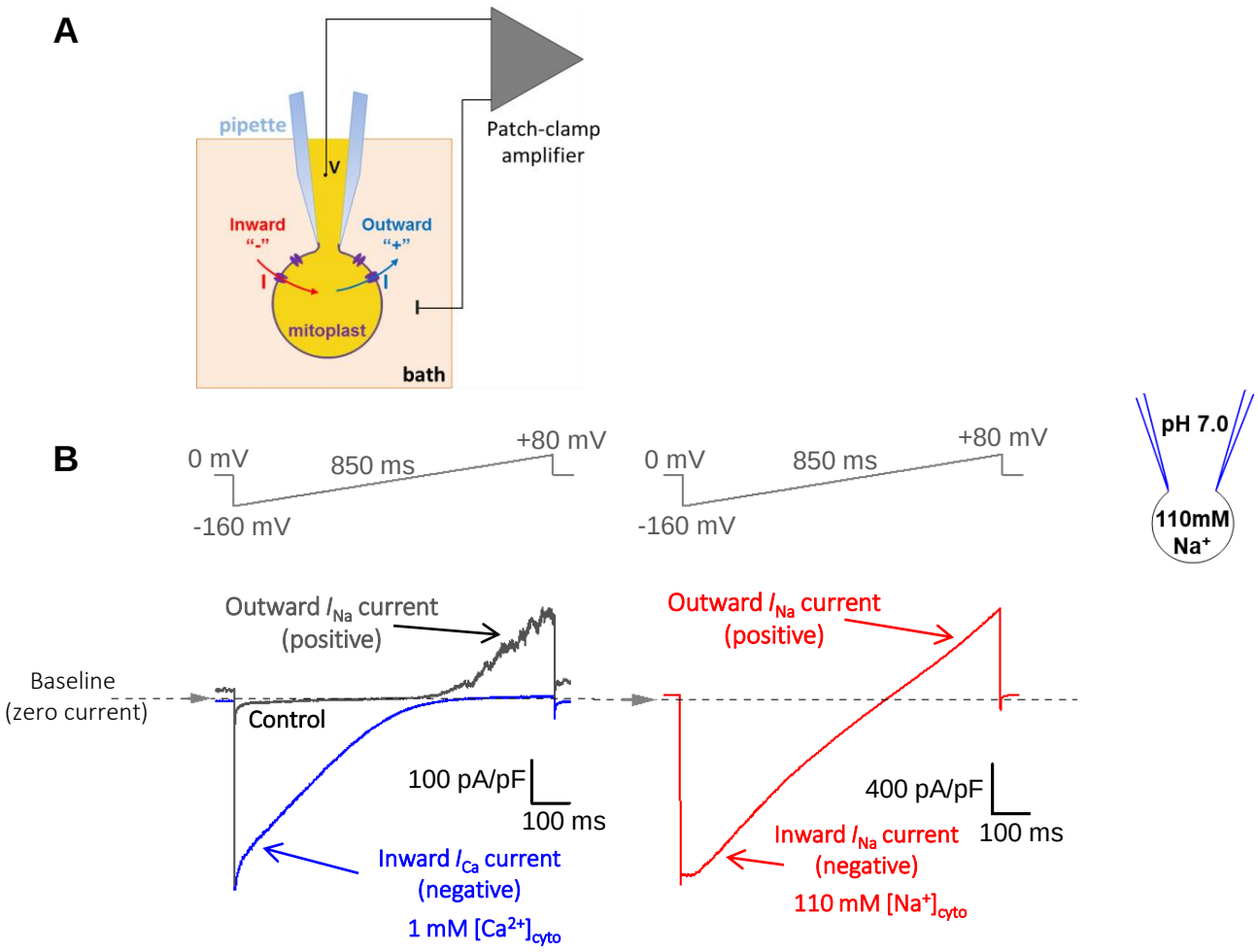
A
pipette
V
Patch-clamp
amplifier
Inward
"-"
Outward
"+"
I
I
I
mitoplast
bath
B
0 mV
850 ms
+80 mV
-160 mV
0 mV
850 ms
+80 mV
-160 mV
pH 7.0
110mM
Na+
Outward I_{Na} current
(positive)
Baseline
(zero current)
Control
100 pA/pF
100 ms
Inward I_{Ca} current
(negative)
1 mM $[Ca^{2+}]_{cyto}$
Outward I_{Na} current
(positive)
400 pA/pF
100 ms
Inward I_{Na} current
(negative)
110 mM $[Na^+]_{cyto}$

Fig. S3

Fig. S4. Protein expression of MCU subunits in MEFs and isolated mitoplasts. (**A**) Co-immunoprecipitation of the MCU complex proteins from mitochondrial and mitoplast fractions. Anti-FLAG beads were used to immunoprecipitate MCU-FLAG (expressed in *MCU*$^{-/-}$ cells) from mitochondrial and mitoplast fractions. Mitochondria isolated from *WT* cells (No FLAG tag) were used as negative control. Left three lanes are protein-complexes immunoprecipitated with anti-FLAG beads. Lane-1: immunoprecipitate (IP) from MCU-FLAG mitochondrial (Mt) lysate, lane-2: IP from MCU-FLAG mitoplast (Mp) lysate, lane-3: IP from *WT* mitochondrial lysate. Right three lanes correspond to samples from the flow-through fraction after immunoprecipitation. Lane-1*: mitochondrial lysate from MCU-FLAG, lane-2*: mitoplast lysate from MCU-FLAG, lane-3*: mitochondrial lysate from *WT*. Upper (MICU1, MCU and EMRE) and lower (MICU2 and TOM20) boxes are from the same samples run on different gels. (**B**) Western blots of protein lysates from cells with *WT* MCU complex (*WT*), *MCU*$^{-/-}$ cells, and *MCU*$^{-/-}$ cells overexpressing MCU (MCU-OE) using anti-MCU and anti-TOM20 (the mitochondrial loading control). (**C**) Western blots of protein lysates from *WT* cells, *EMRE*$^{-/-}$ cells, and *EMRE*$^{-/-}$ cells overexpressing EMRE (EMRE-OE) using anti-EMRE, anti-TOM20 and anti-HSP60 (the mitochondrial loading controls).

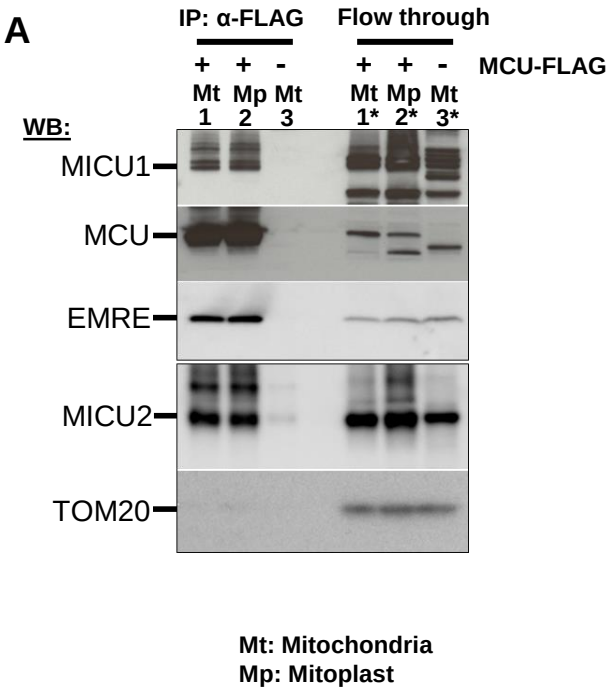
A
IP: α-FLAG
Flow through
+ + - + + -
MCU-FLAG
Mt 1
Mp 2
Mt 3
Mt 1*
Mp 2*
Mt 3*
WB:
MICU1
MCU
EMRE
MICU2
TOM20
Mt: Mitochondria
Mp: Mitoplast

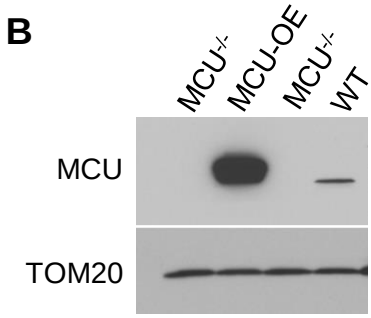
B
MCU-/-
MCU-OE
MCU-/-
WT
MCU
TOM20

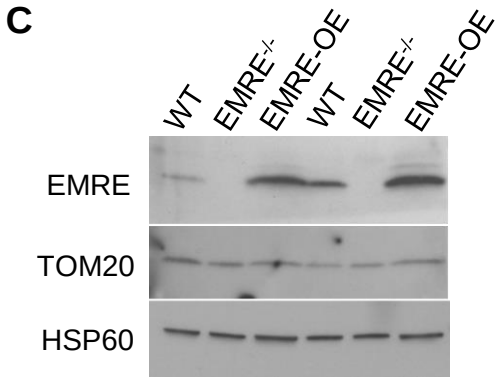
C
WT
EMRE-/-
EMRE-OE
WT
EMRE-/-
EMRE-OE
EMRE
TOM20
HSP60

Fig. S4

Fig. S5. I_{Ca} in MICU1–3 knockouts. (**A**) I_{Ca} amplitude in *WT* and MICU1-3 knockouts measured at -160 mV using 10 μM $[Ca^{2+}]_{cyto}$ with an enlarged Y-axis. Data is same as used in Fig. 1E. Mean ± SEM; one-way ANOVA with post-hoc Tuckey test; $^{**}p < 0.01$. (**B**) Representative inward I_{Ca} in *WT*, *MICU1*$^{-/-}$, *MICU2*$^{-/-}$ and *MICU3*$^{-/-}$ mitoplasts exposed to 5 mM, and 25 mM $[Ca^{2+}]_{cyto}$. (**C**) I_{Ca} amplitude measured at -80 mV in *WT* (n = 13), *MICU1*$^{-/-}$ (n = 14), *MICU2*$^{-/-}$ (n = 8) and *MICU3*$^{-/-}$ (n = 9) mitoplasts at 10 μM, 100 μM and 1000 μM $[Ca^{2+}]_{cyto}$ (*left*, for I_{Ca} traces see Fig. 2A) and at 5 mM and 25 mM $[Ca^{2+}]_{cyto}$ (*right*, for I_{Ca} traces see Figure 1D). Mean ± SEM; one-way ANOVA with post-hoc Tuckey test; $^{***}p < 0.001$.

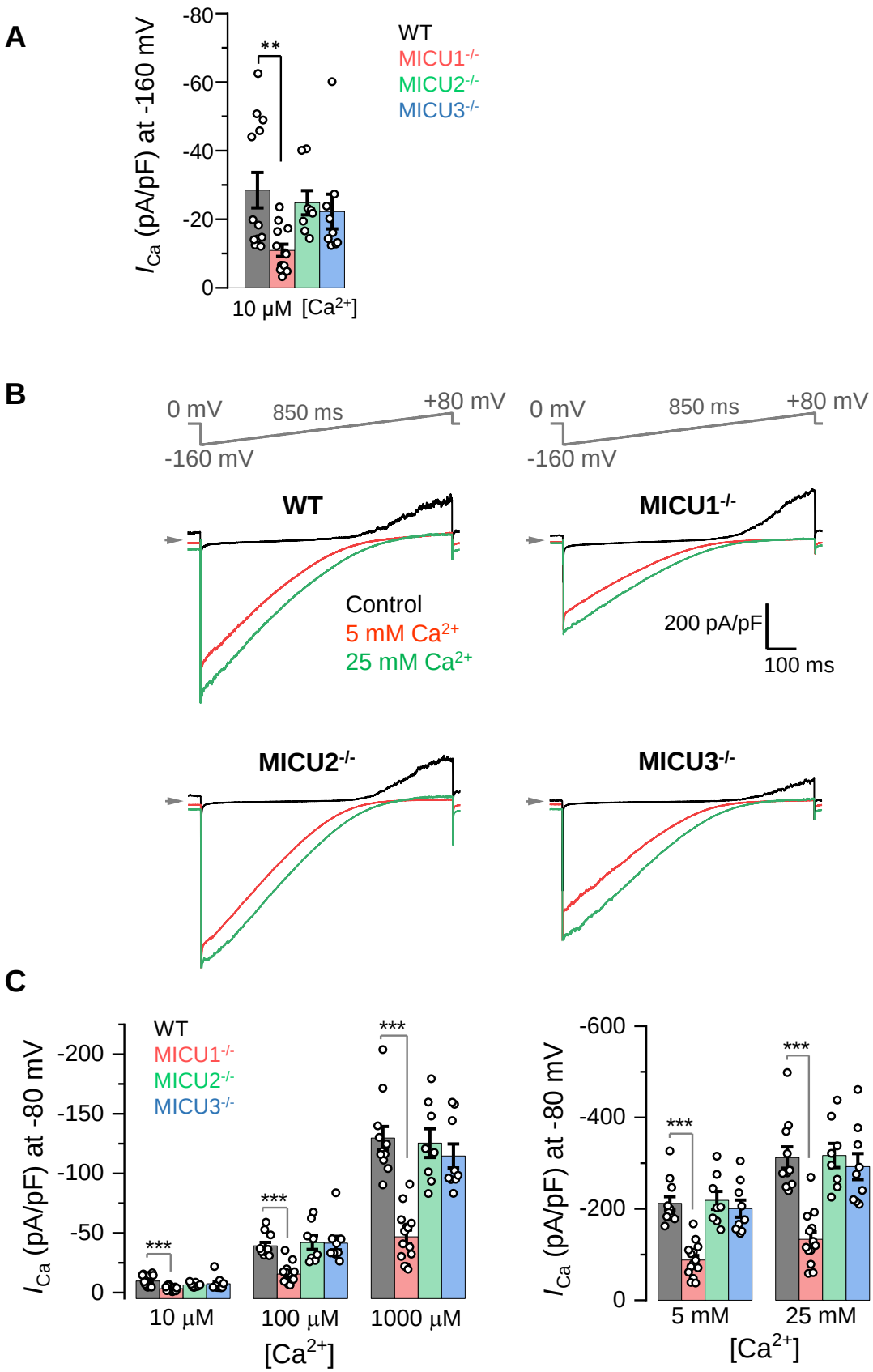
A
-80
-60
-40
-20
0
I_{Ca} (pA/pF) at -160 mV
**
WT
MICU1-/-
MICU2-/-
MICU3-/-
10 μM [Ca2+]
B
0 mV
850 ms
+80 mV
-160 mV
WT
Control
5 mM Ca2+
25 mM Ca2+
MICU1-/-
200 pA/pF
100 ms
MICU2-/-
MICU3-/-
C
-200
-150
-100
-50
0
I_{Ca} (pA/pF) at -80 mV
WT
MICU1-/-
MICU2-/-
MICU3-/-
***
10 μM
100 μM
1000 μM
[Ca2+]
-600
-400
-200
0
5 mM
25 mM

Fig. S5

Fig. S6. Rescue of EMRE expression in *MICU1*$^{-/-}$ does not rescue I_{Ca}. (**A** to **C**) Western blots showing the expression levels of EMRE (A), MCU (B) and MCUb (C) in cells with *WT* MCU complex and *MICU1*$^{-/-}$ (*n* = 3 independent samples each). (**D**) (*Left*) Western blots showing EMRE protein level in *WT* and *MICU1*$^{-/-}$ (before and after EMRE overexpression). (*Right*) Graph represents quantification of Western blot (*n* = 4 independent samples each). (**E**) Representative inward I_{Ca} in *WT*, *MICU1*$^{-/-}$, and when EMRE was overexpressed in *MICU1*$^{-/-}$ (*MICU1*$^{-/-}$ + EMRE) upon exposure to 100 μM and 1000 μM $[Ca^{2+}]_{cyto}$. (**F**) I_{Ca} amplitudes measured at -160 mV in *MICU1*$^{-/-}$ overexpressing EMRE (*MICU1*$^{-/-}$ + EMRE, *n* = 8) as well as in *MICU1*$^{-/-}$ and *WT*. *WT* and *MICU1*$^{-/-}$ data are the same as in Fig. 1E. Mean ± SEM; one-way ANOVA with post-hoc Tuckey test. **p*< 0.05; ***p*< 0.01; ****p*< 0.001.

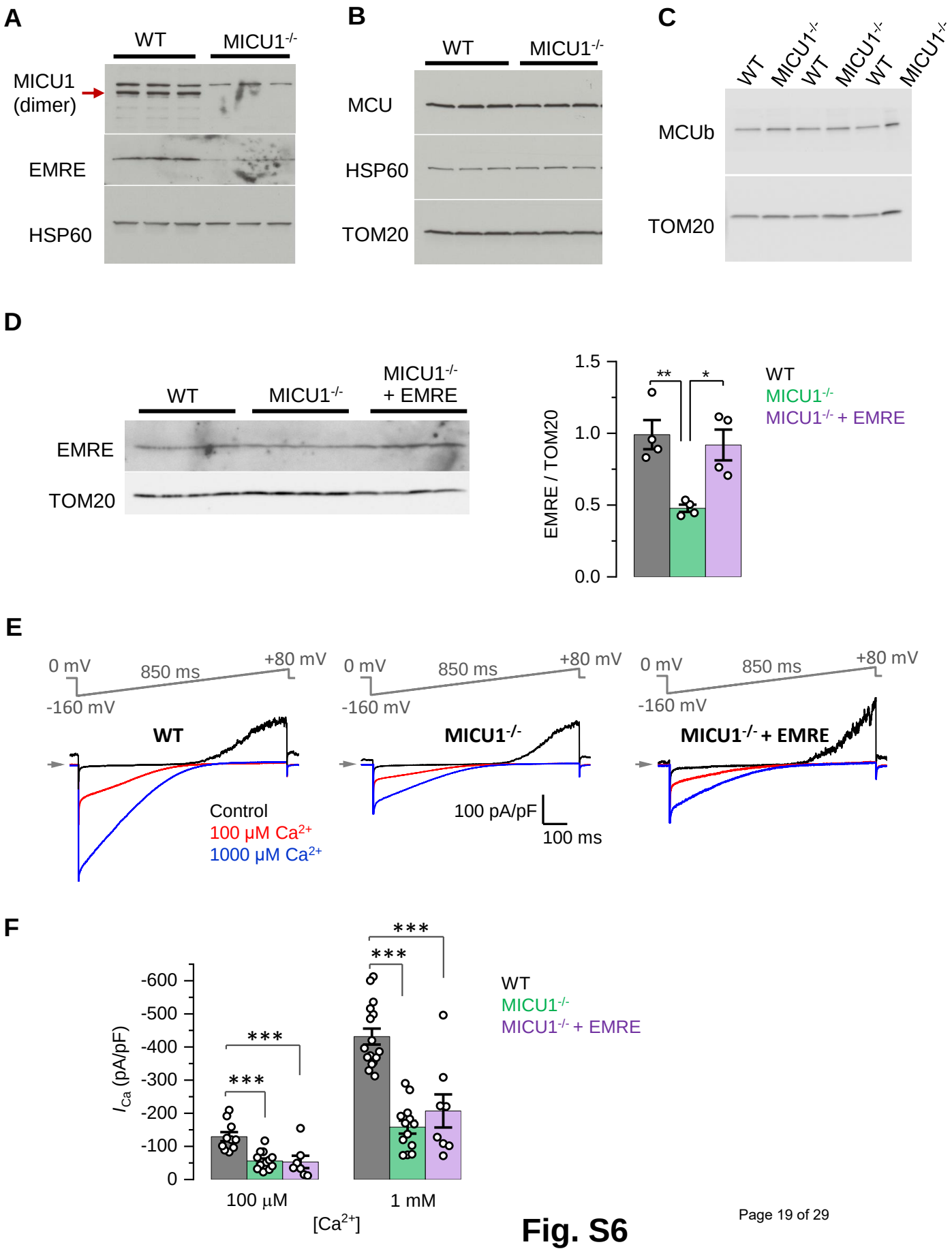
A
WT
MICU1-/-
MICU1 (dimer)
EMRE
HSP60
B
WT
MICU1-/-
MCU
HSP60
TOM20
C
WT
MICU1-/-
WT
MICU1-/-
WT
MICU1-/-
MCUb
TOM20
D
WT
MICU1-/-
MICU1-/- + EMRE
EMRE
TOM20
EMRE / TOM20
1.5
1.0
0.5
0.0
**
*
WT
MICU1-/-
MICU1-/- + EMRE
E
0 mV
850 ms
+80 mV
-160 mV
WT
MICU1-/-
MICU1-/- + EMRE
Control
100 µM Ca2+
1000 µM Ca2+
100 pA/pF
100 ms
F
ICa (pA/pF)
-600
-500
-400
-300
-200
-100
0
***
***
***
***
WT
MICU1-/-
MICU1-/- + EMRE
100 µM
1 mM
[Ca2+]

Fig. S6

Fig. S7. Drp1 does not affect the currents mediated by the MCU complex or their phenotype in *MICU1*$^{-/-}$. (**A**) I_{Ca} amplitudes at -160 mV (*left*) and -80 mV (*right*) in mitoplasts from MEFs with Drp1 (*Drp*$^{+/+}$) and without Drp1 (*Drp1*$^{-/-}$). (n = 17-19) Mean ± SEM. (**B**) I_{Na} amplitudes at -160 mV (*left*) and -80 mV (*right*) in mitoplasts from MEFs with Drp1 (Drp$^{+/+}$, n = 8) and without Drp1 (*Drp1*$^{-/-}$, n = 21). Mean ± SEM. (**C** to **F**) Current phenotypes of *MICU1*$^{-/-}$ in mitoplasts isolated from MEFs with an intact Drp1. (C) Representative I_{Ca} (*blue*) and I_{Na} (*red*) recorded from the *WT* (n = 7) and *MICU1*$^{-/-}$ (n = 12) mitoplasts exposed to 1 mM $[Ca^{2+}]_{cyto}$ or 110 mM $[Na^{+}]_{cyto}$. Amplitudes of I_{Na} (D) and I_{Ca} (E) measured at -80 mV. (F) Ratio between I_{Ca} and I_{Na} measured in the same mitoplast. Mean ± SEM; unpaired t-test, two-tailed; ***p< 0.001.

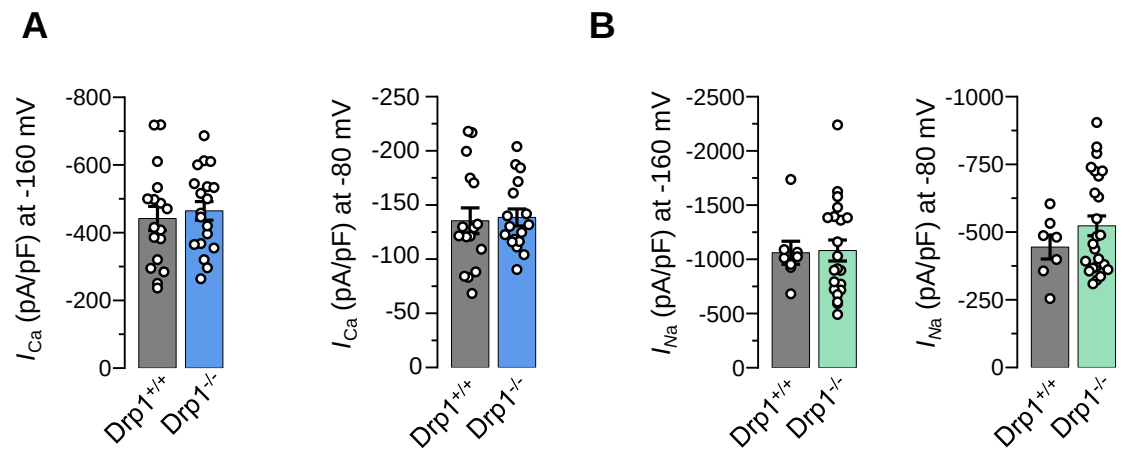

Mitoplasts from MEFs with intact Drp1

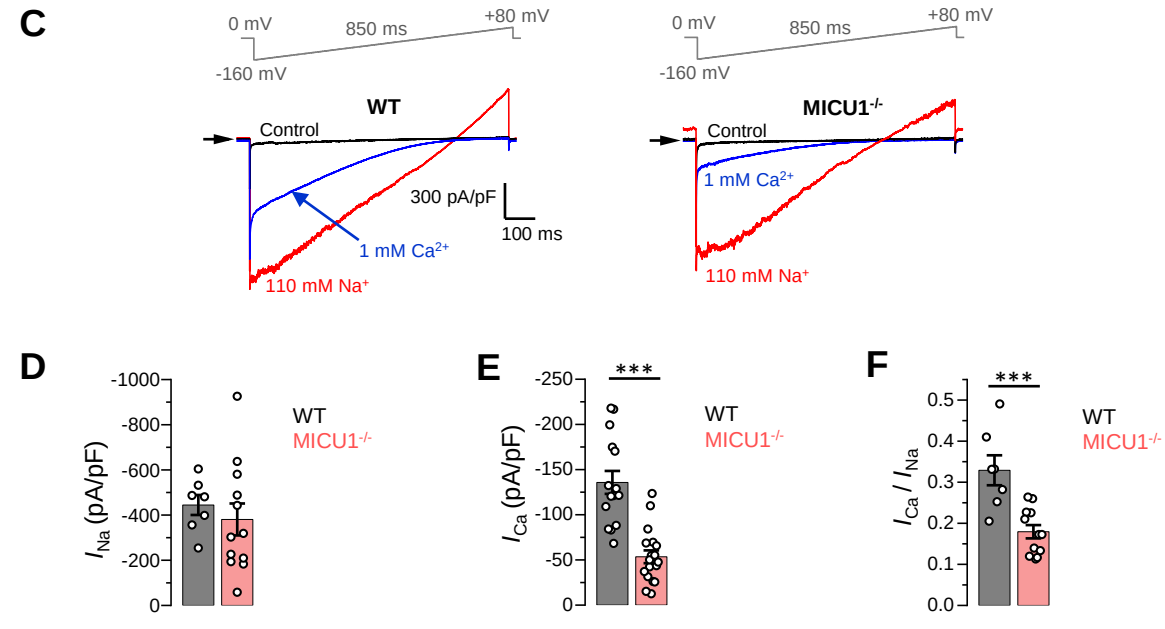

Fig. S7

Fig. S8. Expression levels of different MCU subunits in *MICU2*$^{-/-}$ MEFs and the open probability of MCU at different potentials. (**A** to **C**) Western blots showing the expression levels of MICU2 (A), MCU, EMRE, MICU3 (B) and MICU1 dimers (C) in *WT* and *MICU2*$^{-/-}$ cells (n = 3–6 independent samples each). For detection of MICU1 dimers, samples were prepared in Laemmli buffer without β-mercaptoethanol.

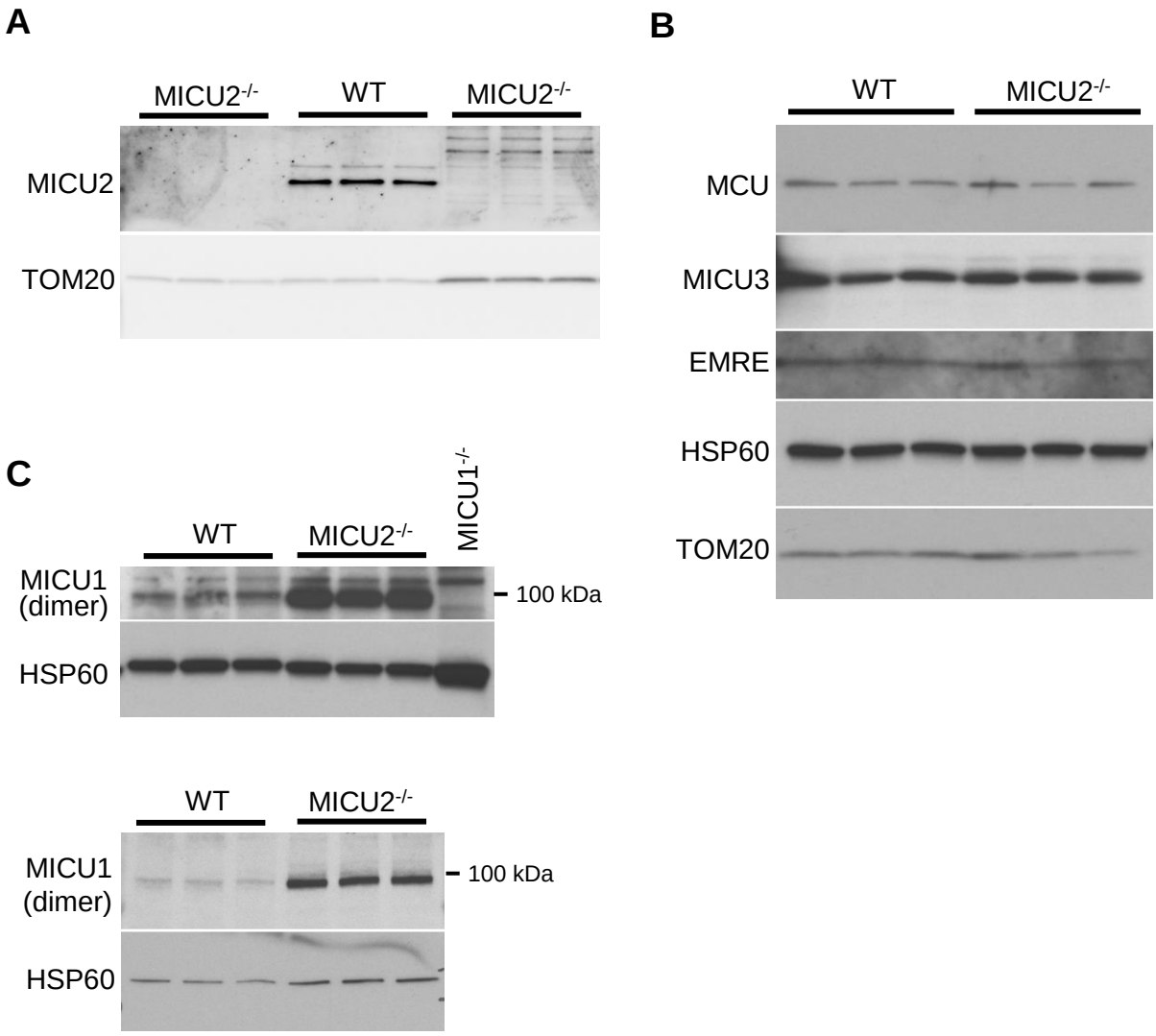
A
MICU2-/-
WT
MICU2-/-
MICU2
TOM20
B
WT
MICU2-/-
MCU
MICU3
EMRE
HSP60
TOM20
C
WT
MICU2-/-
MICU1-/-
MICU1
(dimer)
100 kDa
HSP60
WT
MICU2-/-
MICU1
(dimer)
100 kDa
HSP60

Fig. S8

Fig. S9. Matrix Ca^{2+} does not inhibit I_{Ca}. (*Upper Panels*) Inward I_{Ca} in the presence of 0 (*left*), 400 nM (*middle*) and 400 μM (*right*) $[Ca^{2+}]_{mito}$ (pipette solution). $[Ca^{2+}]_{cyto}$ was 100 μM, 1 mM or 5 mM. (*Lower Panel*) I_{Ca} amplitudes at 0 (n=3-5), 400 nM (n=4) or 400 μM (n=3) $[Ca^{2+}]_{mito}$. I_{Ca} was measured at -160 mV and in different $[Ca^{2+}]_{cyto}$ as indicated. Mean ± SEM; one-way ANOVA with post-hoc Tuckey test.

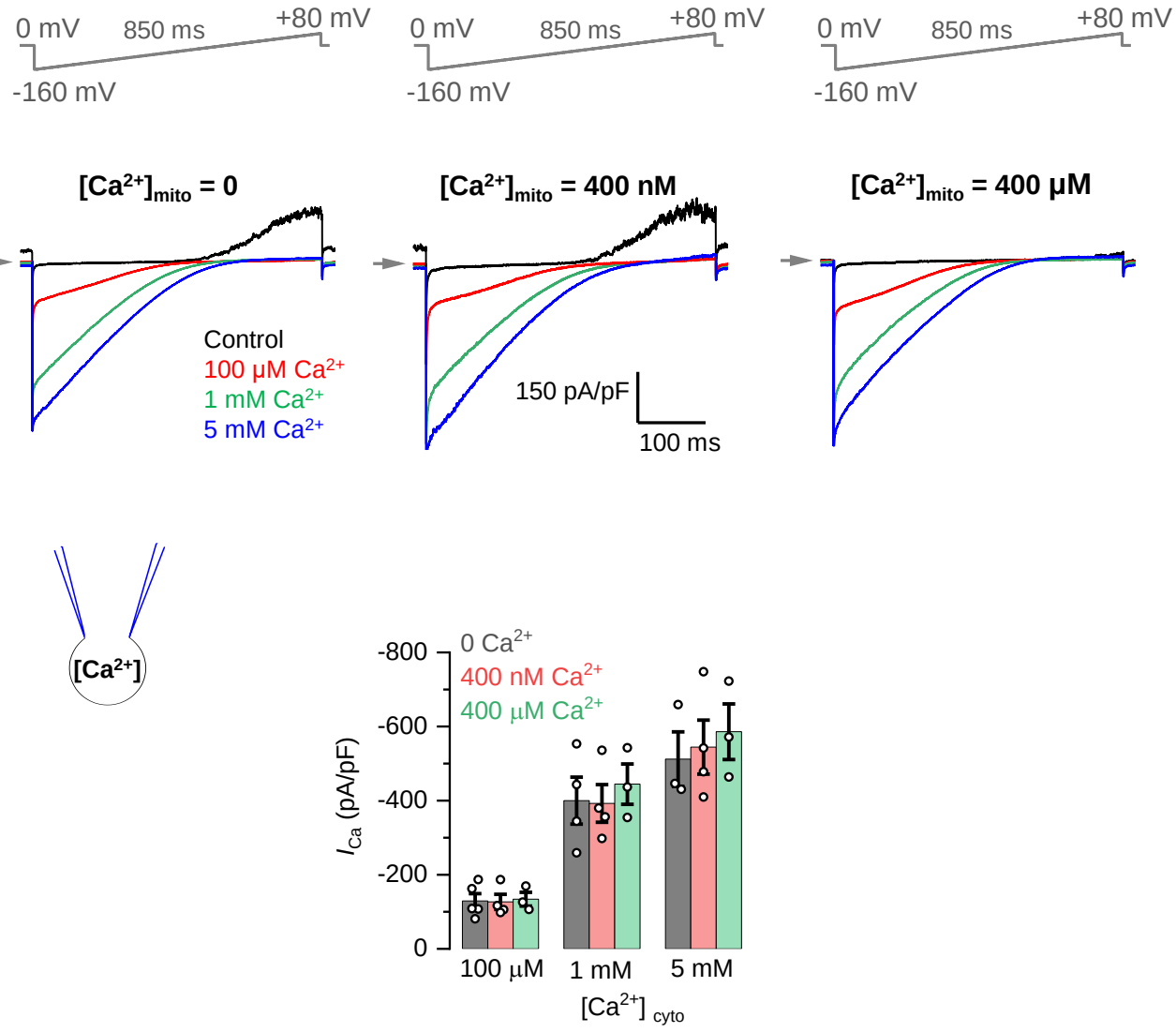
0 mV
850 ms
+80 mV
-160 mV
0 mV
850 ms
+80 mV
-160 mV
0 mV
850 ms
+80 mV
-160 mV
[Ca2+]mito = 0
[Ca2+]mito = 400 nM
[Ca2+]mito = 400 µM
Control
100 µM Ca2+
1 mM Ca2+
5 mM Ca2+
150 pA/pF
100 ms
[Ca2+]
0 Ca2+
400 nM Ca2+
400 µM Ca2+
-800
-600
-400
-200
0
ICa (pA/pF)
100 µM
1 mM
5 mM
[Ca2+] cyto

Fig. S9

Fig. S10. Open probability of the MCU channel in *WT* and *MICU1*$^{-/-}$. (**A** to **C**) Open probability of the MCU channel in *WT* (*n*=5-6) and *MICU1*$^{-/-}$ (*n*=5) at -40 mV (A) -80 mV (B) and at -120 mV (C). The same *WT* and knockout data were used as in Fig. 4D, but presented to show data distribution. Mean ± SEM; unpaired t-test, two-tailed; $^{**}p < 0.01$.

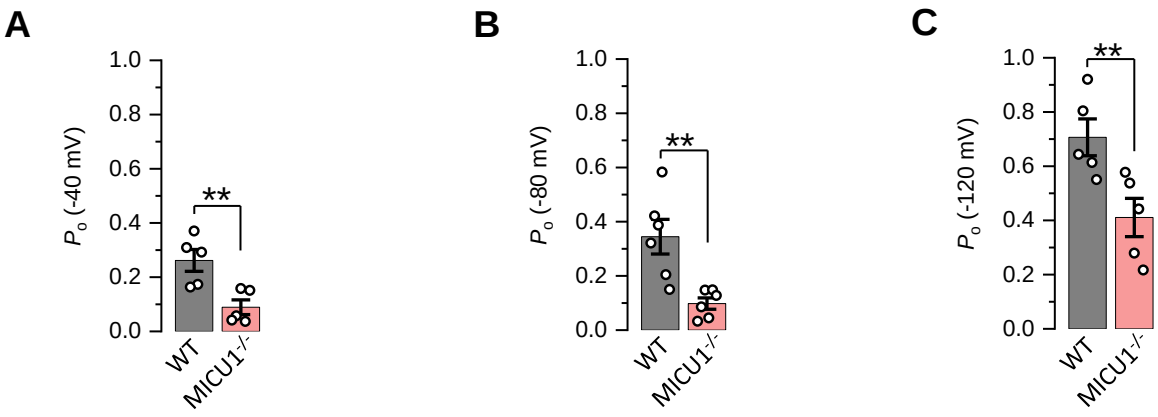

Fig. S10

Table S1. MICU1 effect on MCU as determined by previous electrophysiological experiments.

Citation	MCU current	
	Low $[Ca^{2+}]_{cyto}$	**High $[Ca^{2+}]_{cyto}$**
Hoffman et al., 2013 (*44*)		Inhibition
Patron et al., 2014 (*25*) Lipid bilayer experiments; EMRE subunit, essential for MCU activity and MICU1 interaction, was absent	No effect	Activation
Vais et al., 2016 (*43*)		No change
Kamer et al., 2018 (*42*)		No change

Table S2. MICU1 effect on MCU as determined by previous Ca^{2+} imaging experiments.

Reference	Effect of MICU1 on mitochondrial Ca^{2+} uptake	
	Low $[Ca^{2+}]_{cyto}$	High $[Ca^{2+}]_{cyto}$
Mallilankaraman et al., 2012 (*28*)	Inhibition	No effect
Hoffman et al., 2013 (*44*)	Inhibition	Inhibition
Plovanich et al., 2013 (*23*)		Activation
Csordas et al., 2013 (*29*)	Inhibition	Activation
de la Fuente et al., 2014 (*31*)	Inhibition	Activation
Kamer and Mootha, 2014 (*24*)	Inhibition	
Logan et al., 2014 (*30*)	Inhibition	No effect
Patron et al., 2014 (*25*)	Inhibition	Inhibition
Hall et al., 2014 (*73*)		Inhibition
Antony et al., 2016 (*36*)	Inhibition	Activation
Liu et al., 2016 (*32*)	Inhibition	Activation
Bhosale et al., 2017 (*74*)	Inhibition	
Kamer et al., 2017 (*51*)	Inhibition	
Paillard et al., 2018 (*34*)	Inhibition	Activation
Phillips et al., 2018 (*33*)	Inhibition	